

## Modelling of Refuse-Derived Fuel Gasification Reactor

Márta Kákonyi\*, Ágnes Bárkányi, Tibor Chován, Sándor Németh

Department of Process Engineering, University of Pannonia, 10 Egyetem str., Veszprém, 8200-Hungary  
 kakonyi.marta@mk.uni-pannon.hu

Landfilled municipal solid waste (MSW) emits significant quantities of greenhouse gases (GHG). The gasification process can reduce not only the amount of deposited waste, but also the amount of methane (CH<sub>4</sub>) emitted by landfills. With development of gasification processes, it is possible to chemically convert the waste into useful products, synthesis gas. This energy carrier can be used to generate electricity and produce other valuable materials such as hydrogen, methanol, etc. The raw material of gasification technology is the refused-derived fuel (RDF), which is the non-recyclable part of the MSW. Pyrolytic, oxidation and reduction processes can be separated in the downdraft moving bed reactor type.

The aim of this work is to study the model and the reactions of the pyrolysis and oxidation zone and to investigate whether the model of oxidation zone can be integrated into the model of pyrolysis zone to reduce the computational capacity requirements. RDF pellet sample was milled, and representative samples were studied by thermogravimetric (TG). The kinetic parameters of the reactions were identified. The applied kinetic model can be used to calculate the mass of the produced gas, and a model suitable for determining the gas composition was added. The gas composition was estimated based on the mass balance of the elements. In the first approach, the composition and amount of gas obtained during the simulation of the pyrolysis zone was the raw material of the oxidation zone, then the composition of gas was calculated based on partial oxidation reactions. In the other approach, the gas composition was determined in one step. Both methods provided close to identical composition while the time of computation was almost the same. The biggest relative error in mass balance of the elements was 11.19 % in case of Approach 1 and it was less than 3 % in case of Approach 2.

### 1. Introduction

More than  $5.3 \cdot 10^6$  t of municipal waste is landfilled in the member states of the European Union (European Commission, 2021). Cicuła et al. (2020), based on the IPCC model, determined the amount of methane (CH<sub>4</sub>) generated from the landfilled waste, which was 0.018 t CH<sub>4</sub>/t waste. This value may vary depending on the composition of the waste and the factor associated with the landfill. The CH<sub>4</sub> emission can be 50 m<sup>3</sup>/t of MSW, CH<sub>4</sub> has 25 times the GHG effect of carbon-dioxide (CO<sub>2</sub>) (Yaman et al., 2020). Converting the two CH<sub>4</sub> emissions into CO<sub>2</sub> equivalent (CO<sub>2</sub>eq), they are 0.450 CO<sub>2</sub>eq t/t waste and 0.896 CO<sub>2</sub>eq t/t waste. The gasification plant uses RDF as a raw material, so in addition to diverting waste from the landfill, it also has an impact on carbon reduction. It can reduce GHG emissions from landfill by 96 % while producing energy, synthesis gas. Second-generation biofuels, e.g., hydrogen, or electricity and heat can also be produced from the synthesis gas (Vallejo et al, 2020). The development of gasification technology which produces a valuable product, energy carrier or direct energy from waste can play a major role in climate protection and waste processing. Over the years, several types of gasification reactors have been developed to process coal and biomass. There are also fluid and moving bed, plasma, and rotary kiln reactors (Molina et al., 2016). During the thermal conversion of RDF, the temperature and residence time required for the processing of waste must be ensured.

The downdraft type gasification reactor can be divided into three parts according to the main processes taking place in it: pyrolysis, oxidation, and reduction zones (Salem and Paul, 2018). Several models have been developed to describe the process of pyrolysis at different levels, i.e., reactor, particle, and molecule levels (Hameed et al., 2019). The one-step model, which is the simplest, while keeping low computational demand,

is suitable for the analysis of the results obtained during the TG analysis and identification of the kinetic parameters, as it describes mass conversion. To determine the composition of the pyrolysis zone, Sharma (2011) used empirical relationships for biomass feedstock, which are not applicable for RDF, in this work the estimation is based on the mass balance of elements, including also tar component. In the oxidation zone, the partial oxidation reactions can be described by five reactions (Sharma, 2011). In this paper the two zones were estimated one after another, then in a new approach in one step and the results are compared.

## 2. Experimental

The aim of this work was to investigate the reactions of the pyrolysis and oxidation zone of the downdraft moving bed gasification reactor. Using the so-called one-step kinetic model, the gas mass of the pyrolysis zone can be calculated, but the model is not suitable for determining the gas composition. Based on the ultimate analysis of the raw material and the mass of the elements, the gas composition can be determined with an extrema finder. The results obtained in this step represent the input of the next oxidation zone where the oxidation reactions take place. It was studied that if by modifying the extreme search model and adding a partial amount of oxygen (O<sub>2</sub>) to the pyrolysis zone, the model of two zones can be merged and the simulation time can be shortened. The RDF pellet sample was fine milled and then subjected to TG analysis with a Q-1500 D MOM type derivatograph. Experiments were conducted both in nitrogen (N<sub>2</sub>) and in air atmosphere. The weight of measured sample was 200 g, the heating rate was 10 °C/min for each experiment.

### 2.1 Kinetic parameter identification

The one-step kinetic model was used to describe the mass transformation of the pyrolysis zone (Varhegyi et al., 1994). RDF consists of two raw materials, different plastics, and cellulose. To describe the change in mass, these two main fractions were considered, and kinetic parameters were identified for them. The mass ( $m_i$ ) reduction of the two kinds of raw materials is given by Eq(1), Eq(2) describes the  $y_i$  mass correction factor (Papari and Hawboldt, 2015),  $m_{in,i}$  is the initial mass,  $m_{actual,i}$  is the actual mass and  $m_{final,i}$  is the residue mass. Eq(3) describes the reaction rate constant  $k_i$ ,  $A$  is the pre-exponential factor,  $Ea_i$  is the activation energy,  $R$  is the universal gas constant,  $T$  is the absolute temperature and  $t$  is the time. The total mass ( $m$ ) conversion Eq(4) was recorded as the sum of the conversion of cellulose and plastic. The ratio of cellulose and plastic varies in the raw material.

$$\frac{dm_i}{dt} = -(1 - y_i) \cdot k_i \cdot m_i \quad (1)$$

$$y_i = \frac{m_{in,i} - m_{actual,i}}{m_{in,i} - m_{final,i}} \quad (2)$$

$$k_i = A_i \cdot e^{\frac{-Ea_i}{RT}} \quad (3)$$

$$\frac{dm}{dt} = \frac{dm_c}{dt} + \frac{dm_p}{dt} \quad (4)$$

Kinetic parameters ( $A$  and  $Ea$ ), the ratio of the two raw material fractions, and the residue mass of the fractions were identified with an extrema finder in both atmospheres, for dry feedstock, after reaching a mass constancy from 190 °C. MATLABR2019b software was used, the extrema finder was NOMAD, the objective function to be minimized was the sum of the squares of the difference between the measured and calculated weight percentages (wt.%). The results are shown in Table 1 and Figure 1a in nitrogen and Figure 1b in air atmosphere. The residue of plastic was 3 wt.% in both cases, the residue of cellulose was 51 wt.% in N<sub>2</sub> atmosphere and 20 wt.% in air atmosphere. The ratio of plastic was between 40-51 wt.%. For the N<sub>2</sub> atmosphere, the bottom of the curves is slightly different, which may be caused by an unidentified component. Batch pyrolysis was simulated, with identified parameters, the raw material was 250 g, the moisture content was 17.55 wt.% based on proximate analysis of RDF, the heating rate was 10°C/min. The time of simulation was 3,600 s. Eq(5) was used to describe the drying of the raw material,  $n_w$  is the molar quantity of water in mol,  $k_w$  is calculated with Arrhenius equation Eq(3) (Salem and Paul, 2018). The vapor is treated separately from the mass of the gas. The mass of the gas and amount of the vapor are shown in Figure 2a.

$$\frac{dn_{w,l}}{dt} = -k_w \cdot n_{w,l} \quad (5)$$

Table 1: Identified kinetic parameters

Atmosphere	Fraction	ln(A)	Ea/R (K)	correlation coefficient
Nitrogen	Cellulose	12.13	10 986	0.999
	Plastic	20.29	18 813	0.998
Air	Cellulose	3.58	5 989	0.998
	Plastic	0.1	4 334	0.999

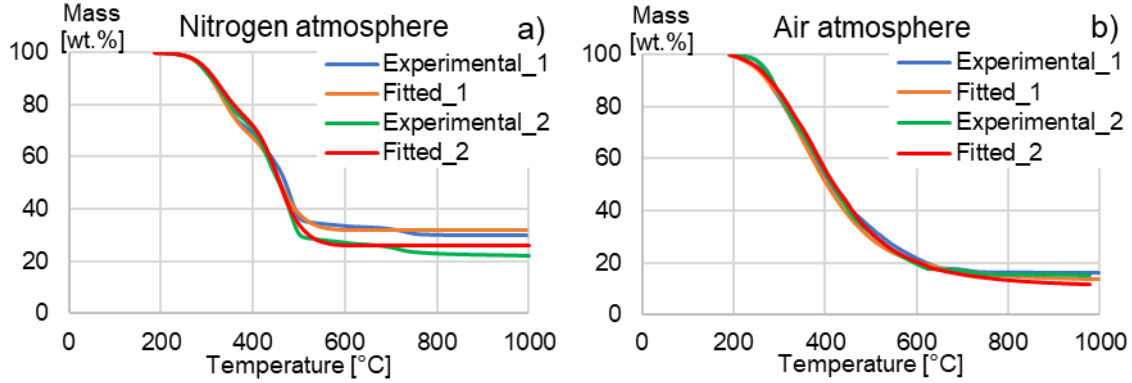


Figure 1: Measured and fitted curves in nitrogen a) and air b) atmosphere

## 2.2 Determination of pyrolysis gas components

In the previous chapter, the result of the calculation was the mass of the gas. Based on ultimate analysis of RDF, the content of carbon, hydrogen, oxygen, ash and pollutant, nitrogen, chlorine, sulfur in the gas can be determined. Empirical relationships are available for biomass gasification, but in the case of RDF they can be used only partially due to the different elemental composition of the feedstock. A different model was needed. An extrema searcher problem was formulated to determine the amount of gas components. Limits of quantities were prescribed based on measurement results (Efika et al., 2015), the parameters  $a$ ,  $b$  and  $c$  refer to the composition of the tar ( $C_aH_bO_c$ ). Ponzio et al. (2006) studied the composition of tar, where the carbon and hydrogen content of the raw material was higher (63.3 wt.% and 8.9 wt.%), the oxygen was lower (20.95 wt.%). In work of Blanco et. al (2012), the oxygen content of the raw material was higher 32.0 wt.%, carbon was 42.7 wt.% and hydrogen content was 6.1 wt.%. Due to the variable composition of the raw material, based on the two papers, the limits of the  $a$ ,  $b$  and  $c$  parameters were determined, the tar could not approximate with a specific average composition. Sharma (2011) used the sum formula  $C_6H_{6.2}O_{0.2}$  to the tar composition, which differs from the C:H:O ratio obtained during the gasification of RDF. The mass of each element ( $m_C$  is mass of carbon,  $m_O$  is mass of oxygen,  $m_H$  is mass of hydrogen) must correspond to the mass of the elements in the components for which inequality constraints have been written (Eq(6)-(8)) allowing a minimal error. In the equations  $M_i$  is the molar masses and  $n_i$  is the moles of components. The extrema finder searched for the minimum difference between the mass of the gas and the mass for each element.

$$0.01 \geq \frac{abs(m_C - M_C \cdot (n_{CO} + n_{CH_4} + n_{CO_2} + a \cdot n_{tar}))}{m_C} \quad (6)$$

$$0.01 \geq \frac{abs(m_O - M_O \cdot (n_{CO} + 2 \cdot n_{CO_2} + n_{H_2O} + c \cdot n_{tar}))}{m_O} \quad (7)$$

$$0.01 \geq \frac{abs(m_H - M_H \cdot (4 \cdot n_{CH_4} + 2 \cdot n_{H_2O} + 2 \cdot n_{H_2} + b \cdot n_{tar}))}{m_H} \quad (8)$$

The  $CH_4$  and  $CO$  content was calculated based on experimental correlation Eq(9)-(10),  $y$  is the mass fraction and  $T$  temperature is in K (Sharma, 2011). The result of the calculation is the molar composition of the gas phase (Figure 2b), which is the input of the oxidation zone.

Table 2: Lower and upper limits of gas components

Limit (wt.%)	CO <sub>2</sub>	H <sub>2</sub> O	H <sub>2</sub>	C <sub>a</sub> H <sub>b</sub> O <sub>c</sub> (Tar)	a	b	c
Lower	10	0	0.04	40	9	16	5
Upper	25	10	0.07	95	10	19	6

$$y_{CO/CO_2} = e^{-1.8447896 + \frac{7730.313}{T} + \frac{5019898}{T^2}} \quad (9)$$

$$y_{CH_4/CO_2} = 5 \cdot 10^{-16} \cdot T^{5.06} \quad (10)$$

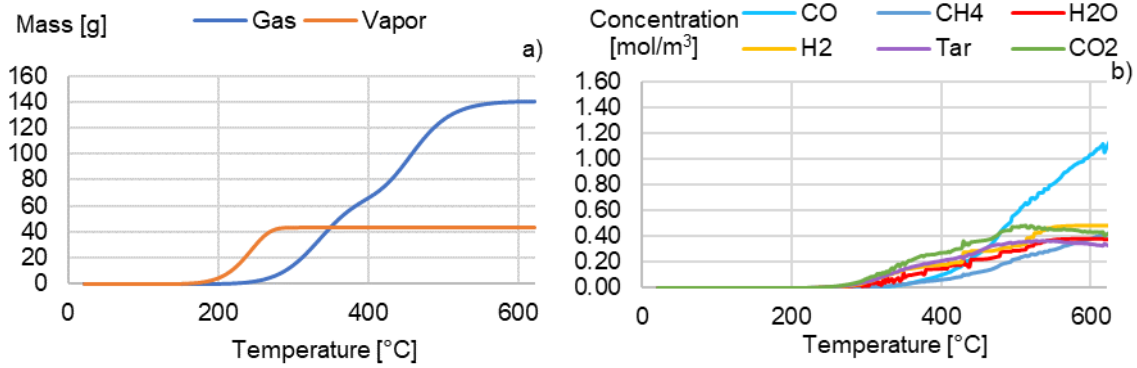


Figure 2: Mass of pyrolysis gas vapor a) and concentration of gas phase of pyrolysis b)

### 2.3 Partial oxidation of pyrolysis gas

Partial oxidation processes have been described by five reactions in Table 3 (Desroches-Ducarne, 1998). The reactions can only be considered one after the other, not in parallel, due to several magnitude differences in the kinetic rate of the reaction. The reactions should be calculated in the order given in Table 3, from R1 to R3, and finally R4 and R5 can be calculated simultaneously (Sharma, 2011).  $C_i$  (mol/m<sup>3</sup>) is the concentration,  $p$  (Pa) is the pressure in the reactor,  $k_i$  is the reaction rate constant,  $T$  (K) is the temperature. The inlet concentrations are the same as those leaving the previous pyrolysis zone. In the case of water, the amount of steam obtained during drying and pyrolysis was summed. The total amount of oxygen fed into the zone was 80 g, the pressure was 10<sup>5</sup> Pa, and the temperature was 800 °C. Batch equipment was simulated. The simulation time was different for each reaction (Figure 3). The longest time was 1 h for the last two reactions (Figure 3d). H<sub>2</sub> (Figure 3a) and CH<sub>4</sub> (Figure 3c) were almost completely converted. The CO content of the pyrolysis gas was burnt in reaction R2 (Figure 3b), and then formed in the following two steps. The simulation time was chosen by the time required for the system to reach its steady state. The step-size was 10<sup>-14</sup> s in case of R1, 10<sup>-5</sup> s in case of R2, 10<sup>-3</sup> s in case of R3, and 1 s in case of R4-R5. The results are shown numerically by weight percentage (wt.%) in Table 4 Approach 1.

Table 3: Oxidation reactions (Desroches-Ducarne, 1998)

Reaction number	Reaction	Reaction rate $r_i$ (mol/m <sup>3</sup> s)	$k_i$
R1	$2H_2 + O_2 \rightarrow 2H_2O$	$k_{H_2} \cdot T^{1.5} \cdot C_{H_2}^{1.5} \cdot C_{O_2}$	$6.73 \cdot 10^7$
R2	$2CO + O_2 \rightarrow 2CO_2$	$k_{CO} \cdot C_{O_2}^{0.5} \cdot C_{H_2O}^{0.5} \cdot C_{CO}$	99.96
R3	$CH_4 + 1.5O_2 \rightarrow CO + H_2O$	$k_{CH_4} \cdot C_{O_2}^{0.8} \cdot C_{CH_4}^{0.7}$	0.26
R4	$C_aH_bO_c + \left(\frac{a}{2} + \frac{b}{4} - \frac{c}{2}\right) O_2 \rightarrow aCO + \frac{b}{2}H_2O$	$k_{tar} \cdot T \cdot p^{0.3} \cdot C_{O_2} \cdot C_{tar}^{0.5}$	$2.88 \cdot 10^{-13}$
R5	$2C + O_2 \rightarrow 2CO$	$k_C \cdot C_{O_2}$	$2.30 \cdot 10^{-5}$

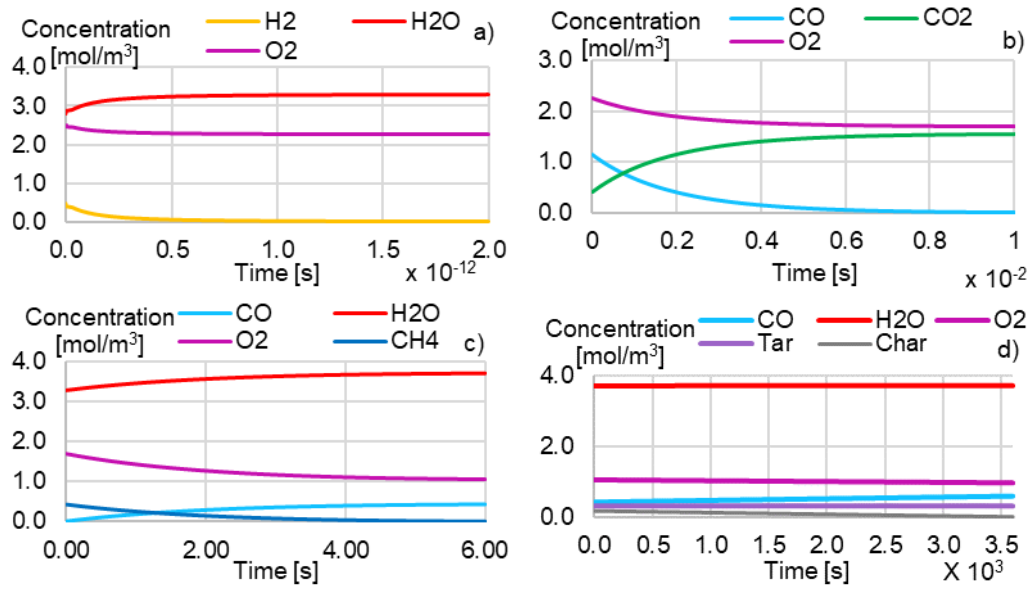


Figure 3: Concentration of gas component after R1 a), after R2 b), after R3 c), after R4 and R5 d)

#### 2.4 Determination of gas composition by integration of the pyrolysis zone

The reduction and oxidation zones have been treated separately in previous studies (Salem and Paul, 2018). In Approach 2, the parameters identified for the results of thermogravimetric analysis in the air atmosphere were used. The aim was to integrate the model of the oxidation zone with that of the pyrolysis zone. The gas mass was calculated with Eq(1)-(5). Based on the results of the oxidation reactions, new constraints were set for the extrema searcher task. Eq(6)-(8) were supplemented by the mass of O<sub>2</sub> ( $m_{O_2,in}$ ) and char ( $m_{Char,in}$ ) fed. They were also added to the mass of the gas for the objective function (Eq(11)-(12)).

$$0.01 \geq \frac{abs(m_C + m_{Char,0} - M_C \cdot (n_{CO} + n_{CH_4} + n_{CO_2} + a \cdot n_{tar} + m_{Char}))}{m_C + m_{Char,0}} \quad (11)$$

$$0.01 \geq \frac{abs(m_O + m_{O_2,in} - M_O \cdot (n_{CO} + 2 \cdot n_{CO_2} + n_{H_2O} + c \cdot n_{tar} + 2 \cdot m_{O_2}))}{m_O + m_{O_2,in}} \quad (12)$$

The conditions, pressure, temperature, and batch process were the same as in the first simulation. The total simulation time was 2 h, as in Approach 1. The result of the simulation is shown in row Approach 2 of Table 4; and the results of the two approaches were compared, the difference in wt.% was calculated. The relative errors are high in some cases, the biggest values are in case of H<sub>2</sub> and CH<sub>4</sub>, however they are negligible or relatively low in case of the main components (CO<sub>2</sub>, CO, H<sub>2</sub>O, Tar, Char). The relative errors for the mass balance of the elements are shown in Table 5. Approach 1 assumes a larger error for elemental O and H. Each difference in mass is less than 3 wt.% in case of Approach 2.

Table 4: Gas composition results after oxidation

Gas component	Unit	CO <sub>2</sub>	CO	H <sub>2</sub>	CH <sub>4</sub>	H <sub>2</sub> O	O <sub>2</sub>	Tar	Char
Approach 1	(wt.%)	26.95	6.63	0.01	0.04	26.28	12.28	27.74	0.08
Approach 2	(wt.%)	26.20	6.61	0.06	0.06	28.02	10.06	28.92	0.07
Relative error	(%)	-2.86	-0.32	76.67	41.79	6.21	-22.07	4.01	-13.71

Table 5: Element errors

Element	Approach 1 relative error (%)	Approach 2 relative error (%)
C	0.74	1.74
H	11.19	-2.77
O	3.63	0.29

### 3. Conclusions

After identifying the kinetic parameters for the two components of the raw material, the gas mass of the pyrolysis zone was determined by the one-step kinetic model. The calculation of the gas composition was formulated as an extrema search problem based on the mass balance of the elements, ensuring the flexibility of the model to the raw material. The molar quantity obtained as a result of the simulation provided the input to the oxidation zone. The partial oxidation reactions were simulated in the appropriate order in different time periods. The result of the gas composition was used to modify the limits of the extrema searcher task. With the kinetic parameters identified for the air atmosphere and the modified extrema searcher model, the pyrolysis and oxidation zone were simulated in one step. The results obtained in the two cases were similar. The aims were to compare the two approaches, and to reduce the computational demand, but the simulation time of the two approaches were similar, in the case of Approach 2 was minimally faster. The experience was that there was no difference between the two solutions, the resource and computational demand were the same. The calculation result was that Approach 2 gives a more accurate result for the element mass balance, the relative error was 1.74 % for C and -2.7 % and 0.29 % for H and O. In case of Approach 1 the relative error of mass balance of C, H and O were 0.74 %, 11.19 % and 3.63 %. Either approach can be integrated in the complex model. Next, expanding the model to the whole reactor and its experimental verification are planned.

### Acknowledgements

The authors would like to acknowledge the staff of the Department of Materials Engineering of the University of Pannonia for performing thermogravimetric measurements. This work was supported by the TKP2020-NKA-10 project financed under the 2020-4.1.1-TKP2020 Thematic Excellence Programme by the National Research, Development and Innovation Fund of Hungary.

### References

- Blanco P. H., Wu C., Onwudili J. A., & Williams P. T., 2012, Characterization of tar from the pyrolysis /gasification of refuse derived fuel: influence of process parameters and catalysis, *Energy & Fuels*, 26(4), 2107-2115.
- Ciuła J., Kozik V., Generowicz A., Gaska K., Bak A., Paździor M., Barbusiński K., 2020, Emission and Neutralization of Methane from a Municipal Landfill-Parametric Analysis, *Energies* 13, 6254.
- Desroches-Ducarne E., Dognier J. C., Marty E., Martin G., Delfosse L., 1998, 'Modelling of gaseous pollutants emissions in circulating fluidized bed combustion of municipal refuse', *Fuel*, 77(13), 1399-1410.
- Efika E. C., Onwudili J. A., Williams P. T., 2015, Products from the high temperature pyrolysis of RDF at slow and rapid heating rates, *Journal of Analytical and Applied Pyrolysis*, 112, 14-22.
- European Commission, Eustat -Municipal Waste by Waste Management Operations <[https://ec.europa.eu/eurostat/databrowser/view/env\\_wasmun/default/table?lang=en](https://ec.europa.eu/eurostat/databrowser/view/env_wasmun/default/table?lang=en)> accessed 07.04.2021.
- Hameed S., Sharma A., Pareek V., Wu H., Yu Y., 2019, A review on biomass pyrolysis models: Kinetic, network and mechanistic models, *Biomass Bioenergy*, 123, 104-122.
- Molino A., Chianese S., Musmarra D., 2016, Biomass gasification technology: The state of the art overview, *Journal of Energy Chemistry*, 25(1), 10-25.
- Papari S., Hawboldt K., 2015, A review on the pyrolysis of woody biomass to bio-oil: Focus on kinetic models, *Renewable and Sustainable Energy Reviews*, 52, 1580-1595.
- Ponzio A., Kalisz S. and Blasiak W., 2006, Effect of operating conditions on tar and gas composition in high temperature air/steam gasification (HTAG) of plastic containing waste, *Fuel Processing Technology*, 87(3), 223-233.
- Salem A. M., Paul M. C., 2018, An integrated kinetic model for downdraft gasifier based on a novel approach that optimises the reduction zone of gasifier, *Biomass and Bioenergy*, 109, 172-181.
- Sharma A.Kr., 2011. Modeling and simulation of a downdraft biomass gasifier 1. Model development and validation, *Energy Conversion and Management*, 52, 1386-1396.
- Vallejo F., Diaz-Robles L., Cubillos F., Espinoza A.P., Espinoza L., Pinilla F., Pino-Cortes E., 2020, Valorization of Municipal Solid Waste using Hydrothermal Carbonization and Gasification: A review, *Chemical Engineering Transactions*, 81, 1045-1050.
- Varhegyi G., Jakab E., Antal M. J., 1994, Is the Broido-Shafizadeh Model for Cellulose Pyrolysis True?, *Energy & Fuels*, 8(6), 1345-1352.
- Yaman C., Anil I., Alagha O., 2020, Potential for greenhouse gas reduction and energy recovery from MSW through different waste management technologies, *Journal of Cleaner Production*, 264, 121432.